An *ab initio* study of $3s$ core-level x-ray photoemission spectra in transition metals

Manabu Takahashi[1] and Jun-ichi Igarashi[2]

[1]*Faculty of Engineering, Gunma University, Kiryu, Gunma 376-8515, Japan*
[2]*Faculty of Science, Ibaraki University, Mito, Ibaraki 310-8512, Japan*

We calculate the $3s$- and $4s$-core-level x-ray photoemission spectroscopy (XPS) spectra in the ferromagnetic and nonmagnetic transition metals by developing an *ab initio* method. We obtain the spectra exhibiting the characteristic shapes as a function of binding energy in good agreement with experimental observations. The spectral shapes are strikingly different between the majority spin channel and the minority spin channel for ferromagnetic metals Ni, Co, and Fe, that is, large intensities appear in the higher binding energy side of the main peak (satellite) in the majority spin channel. Such satellite or shoulder intensities are also obtained for nonmagnetic metals V and Ru. These behaviors are elucidated in terms of the change of the one-electron states induced by the core-hole potential.

I. INTRODUCTION

X-ray spectroscopy has been extensively used for studying electronic properties in solids. Core-level spectroscopy is particularly useful for investigating the electronic states through the dynamical response to the photo-created core-hole. It is well known that the response function in metallic systems exhibits the singular behavior near the Fermi edge.[1–3] In the case of the core-level x-ray photoemission spectroscopy (XPS), the spectra display the asymmetric shapes as a function of binding energy in the vicinity of the threshold.[4] Apart from the edge singularity, some structures have been observed in the high binding-energy region in some ferromagnetic transition metals and their compounds. A notable example is a satellite peak on the $2p$ XPS in ferromagnetic metal Ni, which is located around the region 6 eV higher from the threshold.[5] Feldkamp and Davis[6] analyzed these XPS spectra by evaluating the overlap between the excited states and the ground state, using a numerical method on the linear-combination-atomic-orbital model. They clarified the origin of satellite as a combined effect of the core-hole screening and the interaction between electrons.

As regards the $3s$ XPS, many experiments have already been carried out on ferromagnetic transition metals and their compounds.[7–16] Several materials show satellite or shoulder structures as a function of binding energy, which are interpreted as a result of the $3s$ level splitting due to the exchange interaction between the $3s$ electrons and the valence electrons in the polarized $3d$ states. In some cases, they have been related to the local magnetic moment.[17] On the other hand, having intensively investigated Fe $3s$ XPS in various iron compounds, Acker et al.[8] revealed that only poor correlation exists between the satellite structures and the magnetic moments. They also found that the Fe $3s$ XPS spectra show the satellite structure even in some Pauli paramagnetic compounds. Furthermore, having investigated the Mn and Fe $3s$ XPS spectra in the insulating compounds, Oh et al.[18] concluded that the splitting between and main and satellite

peaks dose not reflect the $3d$ moment when the effect of the charge-transfer becomes important.

We have developed an *ab initio* method to calculate the XPS spectra by extending the theory of Feldkamp and Davis.[6,19] Here we briefly summarize the procedure of calculation. First, we carry out the band structure calculation within the local density functional approximation (LDA) to obtain the one-electron states in the ground state. Next, instead of considering the system with only one core hole in crystal, we consider a system of super-cells with one core-hole per cell. Strictly speaking, we should consider the former system for the XPS event, but the latter system is expected to work better as increasing the cell size. These systems correspond to a kind of impurity problem, where the local charge neutrality has to be satisfied according to the Friedel sum rule.[20] We carry out the band structure calculation based on the LDA, in which the exchange and Coulomb interactions between the core electrons and the conduction electrons and between the conduction electrons are taken into account through the exchange-correlation potential. The charge variation due to screening the core hole in the final states is also taken into account within the super-cell approximation. To guarantee the charge neutrality, we add one extra conduction electron in each super-cell, and seek the self-consistent solution. Then, with the calculated one-electron states, we discretize the momentum space into finite number of points, and construct final states by distributing electrons on these one-electron states. The final state with the lowest excited energy is given by piling the same number of electrons into low energy one-electron levels at each $\mathbf{k}$-point as that in the ground state. We prepare the other final states by creating one electron-hole (e-h) pair, two e-h pairs, and so on. Finally, we calculate the XPS spectra by evaluating the overlaps between thus obtained final states and the ground state with the help of the one-electron wave functions.

The purpose of this paper is to systematically clarify the relation between the spectral shapes and the screening process by calculating the spin resolved $3s$ XPS spec-

tra in a series of ferromagnetic metals Ni, Co, and Fe. The usefulness of our *ab initio* method is demonstrated. We have already reported the spectra in ferromagnetic Fe in Ref. 19. In these metals, spectral shapes have characteristic dependence on elements and spin channels; the spectra have satellite or shoulder in the majority spin channel, while the spectra show single peak structures in the minority spin channel. Here we define the majority (minority) spin channel by the process that the $3s$-core electron is photo-excited to the vacuum state with the same spin as the majority (minority) spin in the conduction band states. As far as we know, such spectra have been analyzed only by using a single band Hubbard model, and has been related to the $3s$-$3d$ exchange interaction.[21] However, the model is, we think, too simple to compare the calculated results quantitatively with the experimental data and to draw definite conclusion.

Applying the *ab initio* method, we calculate the spectra in good agreement with the experimental observations. The screening effects are quite different between the spin channels due to the exchange interaction between the $3d$ electrons and the core hole. The $3d$ states are modified by the core-hole potential at the core-hole site, and sometimes quasi-bound states are created near the bottom of the $3d$ band. The e-h pair excitations from such quasi-bound states to the empty states correspond to the satellite or shoulder intensities. We find that the presence of the quasi-bound states is not sufficient and the $3d$ bands have to be partially occupied in the ground state, in order that the satellite or shoulder structure appears. These considerations well explain the characteristics of the XPS spectra.

Furthermore, to clearly show that the presence of satellite or shoulder has no direct relation to magnetic states, we calculate the $3s$ XPS spectra in nonmagnetic metals V and Cu, and the $4s$ XPS spectra in nonmagnetic metal Ru. We obtain shoulders in the high binding-energy region in V and Ru. On the other hand, we have no such structure in Cu, although the *localized* bound states are clearly created below the bottom of the $3d$ band. We could explain these behaviors in the same way as in the ferromagnetic metals.

The present paper is organized as follows. In Sec. II, we formulate the XPS spectra with the *ab initio* method. In Sec. III, we present the calculated XPS spectra and discuss the behavior. The last section is devoted to the concluding remarks.

II. PROCEDURE OF CALCULATION

A. Formula for XPS spectra

We consider the situation that a core electron is excited to a high energy state with energy ϵ by absorbing an x-ray photon with energy ω_q and that the interaction between the escaping photo-electron and the other electrons could be neglected. The probability of finding a photo-electron

with energy ϵ and spin σ could be proportional to

$$I_\sigma^{\mathrm{XPS}}(\omega_q - \epsilon) =$$
$$2\pi|w|^2 \sum_f |\langle f|s_\sigma|g\rangle|^2 \delta(\omega_q + E_g - \epsilon - E_f), \quad (1)$$

where w represents the transition matrix element from the core state localized at a particular site to the state of photo-electron, and is assumed to be independent of energy ϵ and spin σ. The s_σ is the annihilation operator of a relevant core electron, which is assumed to have only spin σ as the internal degrees of freedom. The kets $|g\rangle$ and $|f\rangle$ represent the ground state with energy E_g and the final state with energy E_f, respectively. We define $|f\rangle$ by excluding the photo-electron. In the following calculation, we replace the δ-function by the Lorentzian function with the full width of half maximum (FWHM) $2\Gamma_s$ with $\Gamma_s = 1.0$ eV in order to take account of the life-time broadening of the core level.

B. Construction of final and initial states

In order to simulate the photo-excited states, we consider a periodic array of super-cells with one core-hole per cell, and calculate the one-electron states by means of the band structure calculation based on the full potential linear augmented plane wave (FLAPW) method. We use the $3 \times 3 \times 3$ bcc super-cell for Fe and V as shown in Fig. 1 in Ref. 19, and the $3 \times 3 \times 3$ fcc super-cell for Co, Ni, Cu and Ru as shown in Fig. 1, where the core-hole sites form a bcc lattice and an fcc lattice, respectively. The larger the unit cell size is, the better results are expected to come out. The $3s$- or $4s$-core states in transition metals are treated as localized states within a muffin-tin sphere, so that we could specify the core-hole site. To ensure the charge neutrality, we assume $n_e + 1$ band electrons per unit cell instead of n_e band electrons, where n_e is the number of band electrons per cell in the ground state. One additional electron per unit cell would not cause large errors in evaluating one-electron states in the limit of large unit-cell size. The self-consistent potential is obtained as the potential for the fully relaxed (screened) state. We write the resulting one-electron state with energy eigenvalue $\epsilon_{\sigma n}(\mathbf{k})$ as

$$\psi_{\sigma n\mathbf{k}}(\mathbf{r}) = \frac{1}{\sqrt{N_c}} \sum_j \phi_{\sigma n\mathbf{k}}(\mathbf{r} - \mathbf{R}_j) \exp(i\mathbf{k} \cdot \mathbf{R}_j), \quad (2)$$

with $\phi_{\sigma n\mathbf{k}}(\mathbf{r}) = u_{\sigma n\mathbf{k}}(\mathbf{r}) e^{i\mathbf{k} \cdot \mathbf{r}}$, where $u_{\sigma n\mathbf{k}}(\mathbf{r})$ has the period of the super-cell, and j runs over N_c super-cells. Needless to say, wave vector $\mathbf{k}$'s have N_c discrete values in the irreducible Brillouin zone. We use these one-electron states as substitutes of the states under a single core-hole. We distribute n_e band electrons per super-cell on these states to construct the excited states. In addition, we carry out the band calculation in the absence of the core-hole with assuming n_e band electrons

per super-cell. The wave function and energy eigenvalue are denoted as $\psi_{\sigma n \mathbf{k}}^{(0)}(\mathbf{r})$ and $\epsilon_{\sigma n}^{(0)}(\mathbf{k})$, respectively. All the lowest $N_e = N_c \times n_e$ levels are occupied in the ground state.

The final states $|f\rangle$'s are constructed by using the one-electron states calculated in the presence of the core-hole in accordance with the following procedure. Defining $n_\sigma^{(0)}(\mathbf{k})$ by the number of levels with spin σ and wave vector $\mathbf{k}$ below the Fermi level in the ground state, we distribute $n_\sigma^{(0)}(\mathbf{k})$ electrons with spin σ and wave vector $\mathbf{k}$ in the states given in the presence of core hole. The final state $|f_0\rangle$ containing no e-h pair is constructed by distributing electrons from the lowest energy level up to the $n_\sigma^{(0)}(\mathbf{k})$'th level with spin σ for each wave vector $\mathbf{k}$. The final states $|f_\nu\rangle$'s containing ν e-h pairs are constructed by annihilating ν electrons in the occupied conduction states and creating ν electrons in the unoccupied conduction states from $|f_0\rangle$.
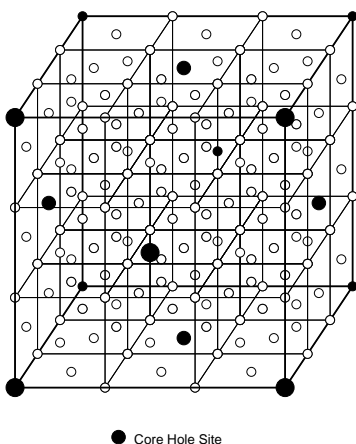

● Core Hole Site

Figure 1: Sketch of a super-cell containing core-holes in fcc structure. Core-hole sites indicated by solid circles are assumed forming a $3 \times 3 \times 3$ fcc lattice. The super-cell for the bcc structure is shown in fig. 1 in Ref. 19.

C. Overlap integrals

We assume that the transition matrix elements between the core state and the photo-excited states are constant. The remaining matrix elements connecting the ground and final states are expressed by

$$\langle f_\nu | s_\sigma | g \rangle = \begin{vmatrix} S_{1,1} & S_{2,1} & ..... & S_{N_e,1} \\ S_{1,2} & S_{2,2} & ..... & S_{N_e,2} \\ .... & .... & .... & .... \\ S_{1,N_e} & S_{2,N_e} & ...... & S_{N_e,N_e} \end{vmatrix}, \quad (3)$$

with

$$S_{i,i'} = \int \phi_i^*(\mathbf{r}) \phi_{i'}^{(0)}(\mathbf{r}) \mathrm{d}^3 r, \quad (4)$$

where the integral is carried out within a unit cell. Subscripts $i = (\sigma, n, \mathbf{k})$ and $i' = (\sigma', n', \mathbf{k}')$ are running over

occupied conduction states in the presence of core hole and in the ground state, respectively. We eliminate the overlaps between the wave functions for the core levels. The corresponding energies difference is given by

$$\Delta E = E_{f_\nu} - E_g$$
$$= E_{f_\nu} - E_{f_0} + E_{f_0} - E_g, \quad (5)$$

where $E_{f_0} - E_g$ includes the energy of core hole, and is treated as an adjustable parameter in the present study such that the threshold of XPS spectra coincides with the experimental value. The excitation energy $E_{f_\nu} - E_{f_0}$ with ν e-h pairs is given by

$$E_{f_\nu} - E_{f_0} = \sum_{(i,j)} (\epsilon_j - \epsilon_i), \quad (6)$$

where ϵ_i's are the Kohn-Sham eigenvalues, and $\epsilon_j - \epsilon_i$ stands for the energy of e-h pair of an electron at level j and a hole at level i. Although the Kohn-Sham eigenvalues may not be proper quasi-particle energies, they practically give a good approximation to quasi-particle energies, except for the fundamental energy gap.[22,23] Substituting Eqs. (3) and (5) into Eq. (1), we obtain the XPS spectra.

In the actual calculation, instead of N_c $\mathbf{k}$-points, we pick up only the Γ point as the sample states for calculating XPS spectra. For Ni, we pick up the X point (and the equivalent Y and Z points) in addition to the Γ point, since the $3d$ band states at the Γ point are fully occupied by both up-spin and down-spin electrons even though the $3 \times 3 \times 3$ fcc super-cell is used.

Before closing this section, we briefly mention the XPS intensity at the energy of threshold. The final state $|f_0\rangle$ with the lowest energy (no e-h pair) has a finite overlap with the ground state $|g\rangle$, giving rise to intensities at the threshold. In principle, such overlap converges at zero with $N_e \to \infty$, according to the Anderson orthogonality theorem.[1] In such infinite systems, energy levels become continuous near the Fermi level and thereby infinite numbers of e-h pairs could be created with infinitesimal excitation energies, leading to the so called Fermi edge singularity in the XPS spectra. The finite contribution obtained above arises from the discreteness of energy levels and could be interpreted as the integrated intensity of singular spectra near the threshold, in consistent with the model calculations for other systems.[6,24]

III. RESULTS AND DISCUSSION

A. Ferromagnetic Transition Metals

In this subsections, we refer to majority(minority) spin as up(down)-spin. The Ni metal takes an fcc structure. For simplicity, the Co metal is assumed to take an fcc structure, although it actually takes an hcp structure.

Table I: Screening electron number in the d-symmetric states inside the muffin-tin sphere at the $3s$ core-hole site. The radii of the muffin-tin spheres are 2.0 Bohr.

	3s hole spin	$\Delta n_{d\uparrow}$	$\Delta n_{d\downarrow}$	$\Delta n_{d\uparrow} + \Delta n_{d\downarrow}$
Fe	up	-1.44	2.38	0.94
	dn	0.47	0.48	0.95
Co	up	-0.52	1.55	1.03
	dn	0.24	0.75	0.99
Ni	up	0.07	0.87	0.94
	dn	0.26	0.65	0.91

The Fe metal takes a bcc structure. Figures 2 and 3 show DOS's projected onto the states with d symmetry (d-DOS) at the core-hole site for Ni and Co, respectively. The corresponding DOS's for Fe are shown in Fig. 3 in Ref. 19. In these calculations, six k-points are picked up in the irreducible Brillouin zone for super-cell systems. The DOS's calculated with no core-hole are essentially the same as those reported by Moruzzi, Janak and Williams.[25] Table I lists the screening electron number $\Delta n_{d\sigma}$ in the d-symmetric states with spin σ, that is, the difference of the occupied electron number between in the presence and in the absence of the core hole inside the muffin-tin sphere.

On the basis of these one-electron states, we calculate the $3s$ XPS spectra, by following the procedure describe in Sec. II. Figures 4, 5 and 6 are the spectra thus calculated as a function of the binding energy $\omega_q - \epsilon$ for Ni, Co, and Fe, respectively, in comparison with the experiments.[10,11,13] The spectral shape in Fig. 6 for Fe is slightly different from our previous result (Fig. 4 in Ref. 19), since the present calculation takes full account of excitations up to three e-h pairs in comparison with only up to two e-h pairs in Ref. 19. The spectra are strikingly different between the up-spin channel and the down-spin channel and strongly depend on elements, in good agreement with the experiments. In the following, we explain the origin of these behaviors in relation to one-electron states screening the core hole.
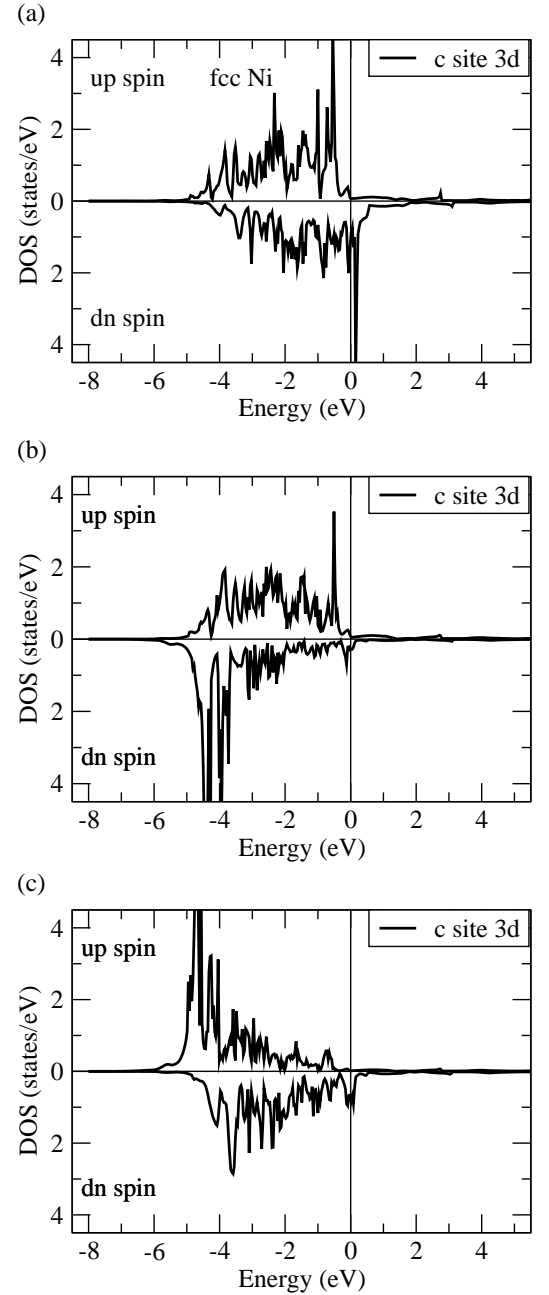

Figure 2: Calculated d-DOS at the core-hole site in the super-cell system in ferromagnetic nickel; (a) d-DOS with no core-hole, (b) d-DOS when the $3s$ up-spin electron is removed, (c) d-DOS when the $3s$ down-spin electron is removed.
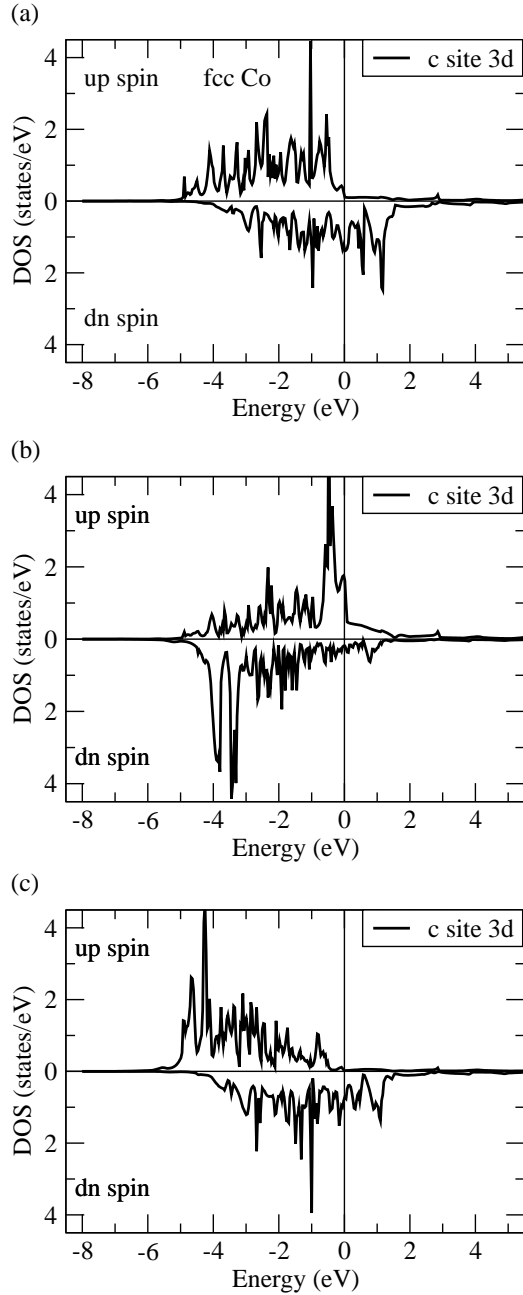
Figure 3: Calculated d-DOS at the core-hole site in the super-cell system in ferromagnetic cobalt; (a) d-DOS with no core-hole, (b) d-DOS when the $3s$ up-spin electron is removed, (c) d-DOS when the $3s$ down-spin electron is removed.

1. Up-spin channel

First we consider the situation that a up-spin $3s$ electron is removed in a unit cell. As shown in Figs. 2 (b) and 3(b), the d-DOS at the core-hole site are strongly modified by the core-hole potential for Ni and Co. The situation is similar to Fe, as shown in Fig. 3 in Ref. 19. The d-DOS's of the down-spin states are strongly pulled down, forming quasi-bound states around the bottom of

Table II: Absolute squares $|A_\uparrow|^2$ and $|A_\downarrow|^2$, where $A_\uparrow$ and $A_\downarrow$ represent the up- and down-spin parts of the overlap integral, respectively, between $|f_0\rangle$ and $s_\sigma|g\rangle$ in the σ-spin channel, that is, $\langle f_0|s_\sigma|g\rangle = A_\uparrow A_\downarrow$.

	up-spin core-hole		dn-spin core-hole	
	$|A_\uparrow|^2$	$|A_\downarrow|^2$	$|A_\uparrow|^2$	$|A_\downarrow|^2$
Ni	0.940	0.234	0.770	0.572
Co	0.983	0.049	0.980	0.601
Fe	0.967	0.127	0.969	0.909

the $3d$ band. On the other hand, the d-DOS's of the up-spin states are slightly pulled down for Ni, and pushed upward to the higher energy region for Co and Fe. The d-DOS's at the site without a core-hole are essentially the same as those in the ground state with no core-hole

Since up-spin electrons are prevented from coming close to the core-hole site due to the exchange interaction with the up-spin core hole, the screening is almost done by down-spin electrons. This tendency is clear in Ni; $\Delta n_{d\downarrow} = 0.87$, while $\Delta n_{d\uparrow} = 0.07$, as shown in Table I. For Co and Fe, the core-hole potential is overscreened by down-spin electrons; $\Delta n_{d\downarrow} = 1.55$(Co), $\Delta n_{d\downarrow} = 2.38$(Fe). This overscreening is compensated by up-spin electrons; $\Delta n_{d\uparrow} = -0.52$(Co), $\Delta n_{d\uparrow} = -1.44$(Fe). As a result, the screening electron numbers become almost unity: 0.94, 1.03, and 0.94 for Ni, Co, and Fe, respectively, indicating that the screening is nearly completed by the d-symmetric states. The magnetic moments at the core-hole site are $-0.2\,\mu_B$, $-0.5\,\mu_B$, and $-1.8\,\mu_B$ for Ni, Co, and Fe, respectively, which are opposite to those without the core-hole, $0.6\,\mu_B$, $1.6\,\mu_B$, $2.1\,\mu_B$, for Ni, Co, and Fe, respectively.

We note that the magnitude of the overscreening by the down-spin electrons becomes weaker Fe, Co, and Ni in that order. In Ni, the number of the down-spin electrons screening the core-hole is just about unity. Consequently, the up-spin $3d$ states become to be less pushed upward to the high energy region in that order. In Ni, the effects of the core-hole potential and the Coulomb repulsion from the screening down electrons subtly cancel out each other and the d-DOS of up-spin states is hardly modified.

It is inferred from these changes in the d-DOS's that one-electron wave functions are largely modified by the core-hole potential particularly for down-spin states. It is necessary to use both the occupied and unoccupied states of the ground state in order to expand those modified one-electron wave functions for the down-spin electrons, since the down-spin $3d$ bands are partially occupied in the ground state. For this reason, the absolute square $|A_\downarrow|^2$ becomes rather small, as shown in table II. Here $A_\uparrow$ $(A_\downarrow)$ represents the the up(down)-spin part of the overlap integral between the lowest-energy final state $|f_0\rangle$ (no e-h pair) and $s_\uparrow|g\rangle$, and thereby $\langle f_0|s_\uparrow|g\rangle = A_\uparrow A_\downarrow$.

The one-electron wave functions for up-spin electrons are also modified from those in the ground state. In spite of such modification, $|A_\uparrow|^2$'s are nearly unity as shown in

Table II. This could be understood as follows. Since the up-spin $3d$ bands are almost fully occupied in the ground state, up-spin one-electron states constituting the final state $|f_0\rangle$ could be represented by a unitary transform of those constituting the ground state $|g\rangle$. Therefore, since the determinant is invariant under unitary transformation, $A_\uparrow$'s are close to unity.

Final states $|f_\nu\rangle$'s containing *up*-spin e-h pairs could give rise to only small intensities, since the states of the excited electrons with up-spin are almost orthogonal to occupied states with up-spin in the ground state $|g\rangle$, and thereby the overlap determinants would vanish. On the other hand, the final states $|f_1\rangle$'s containing one *down*-spin e-h pair could give rise to considerable intensities, since the corresponding one-electron wave functions contain the amplitudes of the unoccupied one-electron states in the ground state $|g\rangle$, and thereby the overlap determinants would not vanish. Considering various combinations of one e-h pair, we obtain intensities distributed in a wide range of binding energy.

to the unoccupied states with down-spin. This excitation may be considered as a core-hole plus d^9, since one of the quasi bound states, which are almost localized at the core-hole site, is empty. In this calculation, however, the states are not split off from the band bottom edge, indicating that the core-hole-dn-hole states are only weakly bound. The satellite binding energy of the calculated spectra is 1 eV smaller than that of the observed spectra. This discrepancy might be owing to the LDA. The Excitations of two e-h pairs would give rise to considerable intensities in the energy range $\omega_q - \epsilon = 110 \sim 120$ eV. Excitations of three e-h pairs give rise to only small intensities.
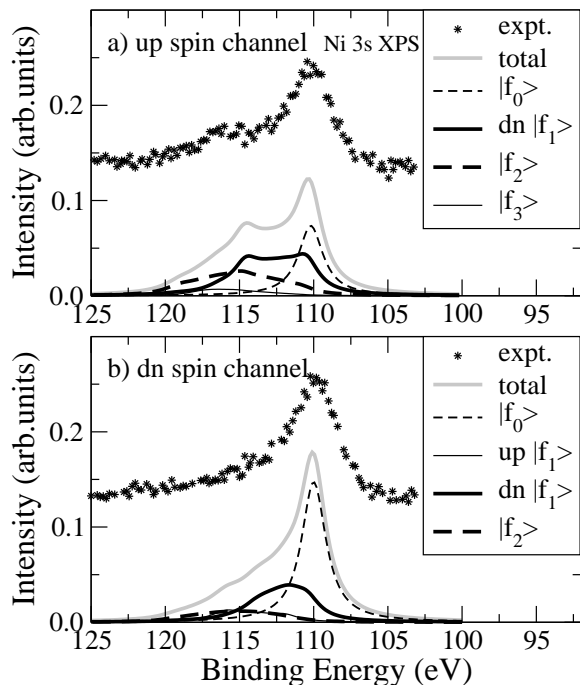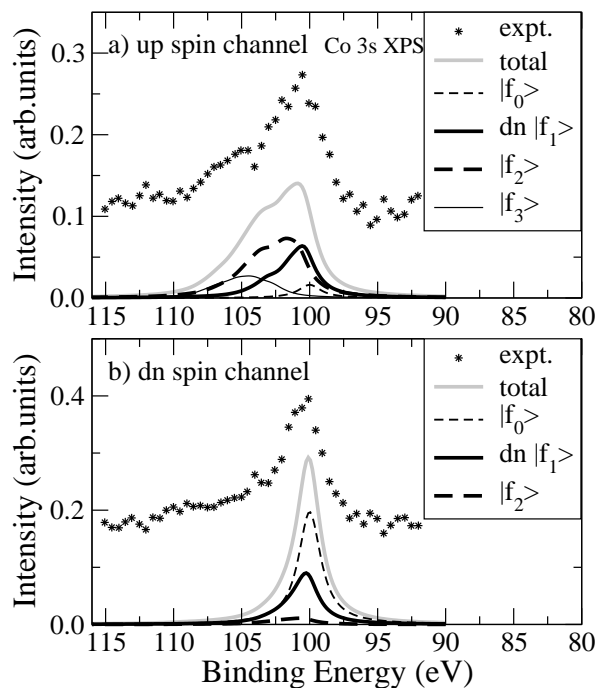

Figure 4: $3s$ XPS spectra in ferromagnetic nickel as a function of binding energy. (a) and (b) are for the up-spin and down-spin channels, respectively. The experimental data are taken from Ref. [13].

Figure 5: $3s$ XPS spectra in ferromagnetic cobalt as a function of binding energy. (a) and (b) are for the up-spin and down-spin channels, respectively. The experimental data are taken from Ref. [10].

Figure 4(a) shows the calculated spectra for Ni in comparison with experimental observations in the up-spin channel. The calculated spectra have maximum intensity at the threshold around $\omega_q - \epsilon = 110$ eV and the significant satellite intensity around $\omega_q - \epsilon = 115$ eV. Note that that the final states containing one down-spin e-h pair give rise to considerable intensities, extending over main and satellite regions. The satellite intensity corresponds to excitations of one e-h pair from the quasi-bound states

Figure 5(a) shows the calculated spectra for Co. The calculated spectra have a broad peak structure with the maximum intensity at the threshold around $\omega_q - \epsilon = 101$ eV. They also have large shoulder intensities around $\omega_q - \epsilon = 104$ eV. The former peak originates from the excitations with one and two e-h pairs. The contribution of the lowest-energy final state $|f_0\rangle$ (no e-h pair) is quite small due to small $|A_\downarrow|^2$. The latter shoulder originates from excitations of two and three e-h pairs, probably including the excitations from the quasi-bound states to the unoccupied states with down-spin.
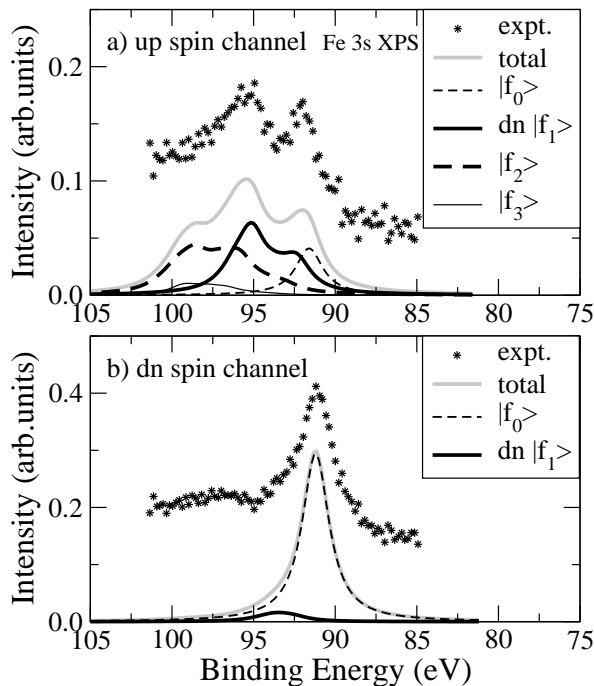
Figure 6: $3s$ XPS spectra in ferromagnetic iron as a function of binding energy. (a) and (b) are for the up-spin and down-spin channels, respectively. The experimental data are taken from Ref. [11].

Figure 6(a) shows the calculated spectra for Fe. The calculated spectra consist of a peak around $\omega_q - \epsilon = 92$ eV and a satellite peak around 95 eV. The satellite peak is larger than the peak around the threshold. The final states $|f_1\rangle$'s containing one down-spin e-h pair give rise to the satellite intensity. The final states $|f_2\rangle$'s containing two e-h pairs give rise to a shoulder to the satellite around $\omega_q = \epsilon = 97 \sim 100$ eV, as shown in the figure. The excitations of three e-h pairs gives rise to finite but small intensities in the wide energy range around 98 eV.

2. Down-spin channel

When a down-spin $3s$ electron is removed in a unit cell, the screening behavior is quite different from the situation where a up-spin $3s$ electron is removed. As shown in Figs. 2(c) and 3(c), and the bottom panel in Fig. 3 in Ref. 19, the d-DOS's at the core-hole site for Ni, Co, and Fe are strongly modified by the core-hole potential. Different from the up-spin channel, the effect is larger for up-spin conduction states than for down-spin conduction states; large weights are transferred to the bottom of the conduction band in the up-spin d-DOS's, while the weights are slightly shifted downward to the lower energy region in the down-spin d-DOS's.

The screening electron numbers are rather smaller in the up-spin state than in the down-spin state, as listed in Table I. This difference arises from the fact that up-spin $3d$ states are almost occupied in the ground state. The

total screening electron numbers are almost unity, 0.91, 0.99, and 0.95 for Ni, Co, and Fe, respectively. The local magnetic moments at the core-hole site are not significantly changed from those in the ground states.

The $|A_\uparrow|^2$'s are not far from unity as listed in Table II, by the same reason as in the up-spin channel. Note that $|A_\downarrow|^2$'s are larger than in the up-spin channel, indicating that one-electron wave functions for down-spin conduction electrons are less modified in the down-spin channel than in the up spin-channel.

Figure 4(b) shows the calculated spectra for Ni, in comparison with the experiment. The final states $|f_1\rangle$'s containing one e-h pair with down-spin give rise to considerable intensities in a wide energy region $110 \sim 115$ eV, while the final states $|f_2\rangle$'s containing two e-h pairs give rise to small intensities in a wide energy region with the maximum around $\omega_q - \epsilon = 115$ eV. We obtain a asymmetric shape with a tail in the high-energy region in agreement with the experiment.

Figure 5(b) shows the calculated spectra for Co. The lowest-energy final states $|f_0\rangle$ gives rise to a peak at the threshold around $\omega_q - \epsilon = 100$ eV. Different from Ni, final states $|f_1\rangle$'s and $|f_2\rangle$'s give rise to intensities on a limited region near the threshold. This suggests that one-electron wave functions are modified only for levels in the vicinity of the Fermi level. Contributions of final states $|f_3\rangle$'s (three e-h pairs) are found negligible.

Figure 6(b) shows the calculated spectra for Fe. The final state $|f_0\rangle$ gives rise to a main peak at the threshold $\omega_q - \epsilon = 91$ eV with the largest contribution in the three metals. Final states $|f_1\rangle$'s with one down-spin e-h pair give rise to a broad peak around 94 eV, which is quite small in comparison with the main peak. Although the observed spectra show small satellite intensity around $\omega_q - \epsilon = 97.5$ eV, the present calculation gives no intensity there. It is unclear on the mechanism giving the intensity to our knowledge.

B. Nonmagnetic metals

In ferromagnetic metals Fe, Co, and Ni, the XPS spectral shapes remarkably depend on the spin channel, owing to the exchange interaction between the core hole and the conduction electrons. Although the spectral shape is found closely related to the filling of band states, the presence of the satellite in the XPS spectra seems to have no direct relation to ferromagnetic states. In this subsection, taking up typical nonmagnetic metals Cu, V and Ru, we clarify this issue. Since the spectra are independent of the spin channel in nonmagnetic metals, we consider the down-spin channel in the following. We assume the fcc structure for Cu and Ru, and the bcc structure for V.

Figure 7 show the d-DOS for Cu. The DOS calculated with no core-hole are essentially the same as those reported by Moruzzi, Janak and Williams.[25] The d-DOS at the core-hole site is shifted downward to the deeper energy region. The localize bound-states are clearly created

below the $3d$ bands in both up- and down-spin states. As listed in Table III, the screening electron numbers are given by $\Delta n_{d\uparrow} = 0.31$, $\Delta n_{d\downarrow} = 0.24$, and the total screening electron number is given by $\Delta n_{d\uparrow} + \Delta n_{d\downarrow} = 0.55$. This indicates that the core-hole potential is not sufficiently screened by the $3d$ electrons at the core-hole site. Here we note that the screening mechanism seems to be somewhat different from the other metals which have partially occupied d-bands and do not show the bound states. Since the $3d$ band states are almost fully occupied in the ground state, the change of the charge density is hardly achieved by a unitary transform of the $3d$ band states. Since the bound states are split off from the band bottom edge, the radial part of the local atomic wavefunctions constituting the bound states at the core-hole site is slightly shrunk compared to that in the ground state with no core-hole, leading to the small change of the charge density. This shrink of radial part of the local atomic wavefunctions cannot be described by a unitary transform of the $3d$ band states in the ground state. The states with much higher energy in the ground state necessarily constitute the bound states to some extent.
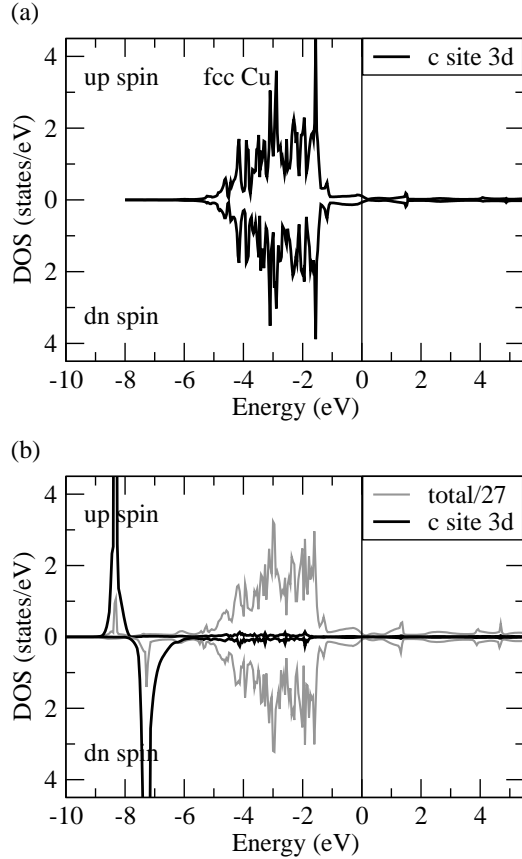
(a)

(b)

Figure 7: (a) DOS calculated in a system of super-cell with no core-hole in nonmagnetic copper. The solid line represents the DOS projected onto the d-symmetry within the muffin-tin sphere. (b) DOS at the site of $3s$ down-spin core-hole. The thin line represents the total DOS divided by the number of atoms in a unit cell.

Figure 8 shows the d-DOS for V. The d-DOS at the core-hole site is shifted downward to the deeper energy region for up-spin states, while the d-DOS is shifted upward for down-spin states. No bound state is formed. As listed in Table III, the screening electron numbers are given by $\Delta n_{d\uparrow} = 1.21$, $\Delta n_{d\downarrow} = -0.21$, and the total number by $\Delta n_{d\uparrow} + \Delta n_{d\downarrow} = 1.00$. The core-hole potential is overscreened by up-spin electrons, and the overscreening is compensated by down-spin electrons. Note that the screening is complete within the $3d$ electrons at the core-hole site. The screening is effective because the $3d$ bands are partially occupied.
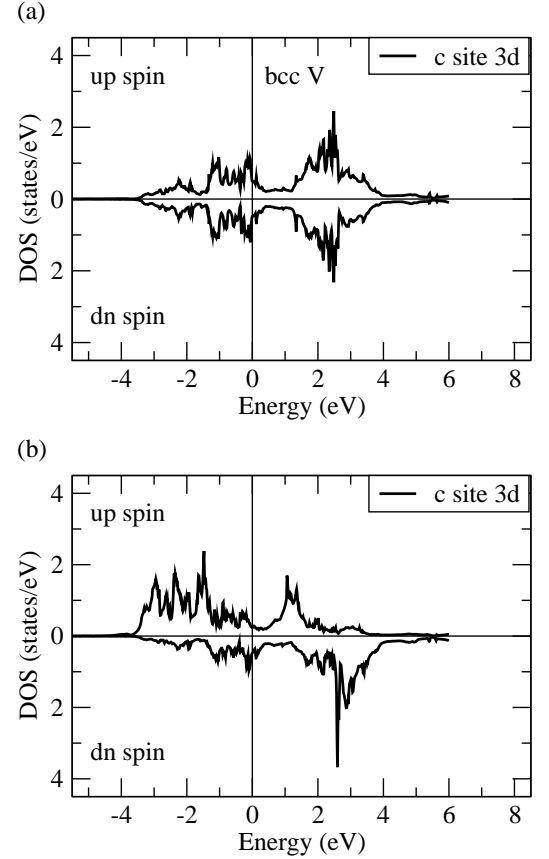
(a)

(b)

Figure 8: (a) DOS calculated in a system of super-cell with no core-hole in nonmagnetic vanadium. The solid line represents the DOS projected onto the d-symmetry within the muffin-tin sphere. (b) DOS at the site of $3s$ down-spin core-hole. The solid line represents the DOS projected onto the d-symmetry within the muffin-tin sphere.

Figure 9 shows the d-DOS for Ru. The d-DOS's at the core-hole site are shifted downward to the deeper energy region with both spin states, but the change is the smallest in the three cases without any bound states. This is probably related to the fact that the $4d$ electrons are more itinerant than the $3d$ electrons. As listed in Table III, the screening electron numbers are $\Delta n_{d\uparrow} = 0.77$, $\Delta n_{d\downarrow} = 0.24$, and $\Delta n_{d\uparrow} + \Delta n_{d\downarrow} = 1.01$, indicating that the screening is nearly completed by the $4d$ electrons
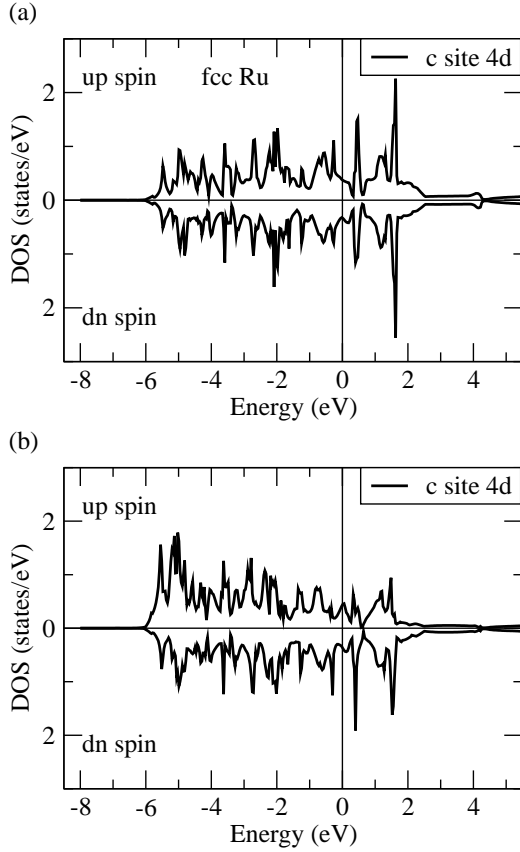
at the core-hole site.

Figure 9: (a) DOS calculated in a system of super-cell with no core-hole in nonmagnetic ruthenium. The solid line represents the DOS projected onto the d-symmetry within the muffin-tin sphere. (b) DOS at the site of $4s$ down-spin core-hole.

Table III: Screening electron number with respect to the d symmetry within the muffin-tin sphere at the $3s$ ($4s$) down-spin core-hole site. The radii of the muffin-tin spheres are 2.0, 2.1, and 2.3 Bohr for Cu, V, and Ru, respectively.

	3s hole spin	$\Delta n_{d\uparrow}$	$\Delta n_{d\downarrow}$	$\Delta n_{d\uparrow} + \Delta n_{d\downarrow}$
Cu	dn	0.31	0.24	0.55
V	dn	1.44	−0.44	1.00
Ru	dn	0.77	0.24	1.01

We calculate the up- and down-spin parts of overlap integrals between the lowest-energy final state $|f_0\rangle$ and the ground state $|g\rangle$, which values are listed in Table IV.

Table IV: Absolute squares $|A_\uparrow|^2$ and $|A_\downarrow|^2$, where $A_\uparrow$ and $A_\downarrow$ represent the up- and down-spin parts of the overlap integral between $|f_0\rangle$ and $s_\downarrow|g\rangle$, that is, $\langle f_0|s_\downarrow|g\rangle = A_\uparrow A_\downarrow$.

	dn-spin core-hole	
	$|A_\uparrow|^2$	$|A_\downarrow|^2$
Cu	0.910	0.935
V	0.571	0.938
Ru	0.681	0.949

For Cu, $|A_\uparrow|^2$ and $|A_\downarrow|^2$ are close to unity, although the one-electron wave functions are strongly modified. Since the $3d$ bands are fully occupied in the ground state, one-electron wave functions constituting $|f_0\rangle$ are nearly expressed by a unitary transform of those constituting $|g\rangle$, except for the shrink of the radial part of the atomic wavefunctions at the core-hole site. Therefore, the squares of the overlap determinant $|A_\uparrow|^2$ and $|A_\downarrow|^2$ are nearly unity. Final states $|f_1\rangle$ (one e-h pair), $|f_2\rangle$ (two e-h pairs), and so on, could have merely very small overlaps with $s_\downarrow|g\rangle$, since the one-electron state on which the excited electron sits is nearly orthogonal to the one-electron states constituting the ground state. Thus we have a simple single peak structure coming from $|f_0\rangle$ without any noticeable intensities on the higher binding energy side, as shown in Fig. 10. This result is consistent with the experimental observation.[7] Note that the change of the wave functions is not directly related to the spectral shape. The effect due to forming strong bound states is not seen.
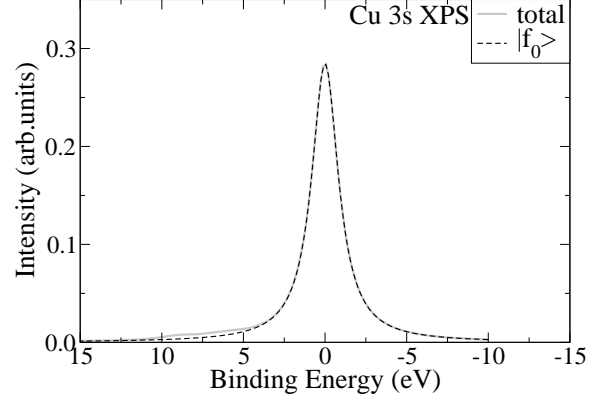

Figure 10: $3s$ XPS spectra in nonmagnetic copper as a function of binding energy in the down-spin channel.

For V, $|A_\downarrow|^2$ is close to unity. This suggests that one-electron wave functions for down-spin electrons are little modified from those in the ground state. On the other hand, $|A_\uparrow|^2$ is rather smaller than unity. This suggests that up-spin one-electron wave functions constituting $|f_0\rangle$ include the amplitudes of the unoccupied one-electron states in the ground state. In such a situation, the final states $|f_1\rangle$'s containing one e-h pair with up-spin could have finite overlaps with the ground state. Figure 11

shows the calculated spectra. We have a main peak coming from the final state $|f_0\rangle$ at the threshold and the noticeable shoulder coming from the final states $|f_1\rangle$'s.
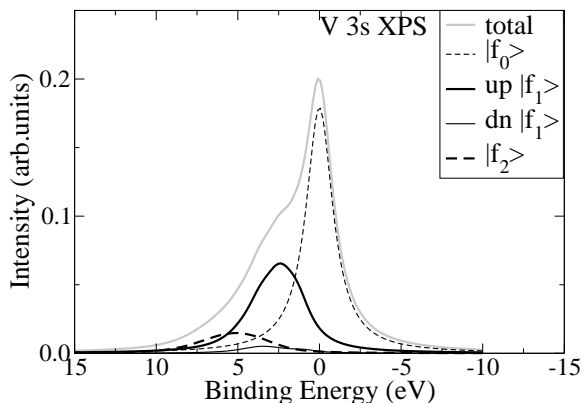

Figure 11: $3s$ XPS spectra in nonmagnetic vanadium as a function of binding energy in the down-spin channel.

For Ru, $|A_\downarrow|^2$ is again close to unity by the same reason as in V. The $|A_\uparrow|^2$ is smaller than unity, although it is larger than that in V. This indicates that one-electron wave functions constituting $|f_0\rangle$ are less modified by the core-hole potential in comparison with V. Final states $|f_1\rangle$'s containing one e-h pair with up-spin give rise to a shoulder structure with a little smaller intensity than in V.
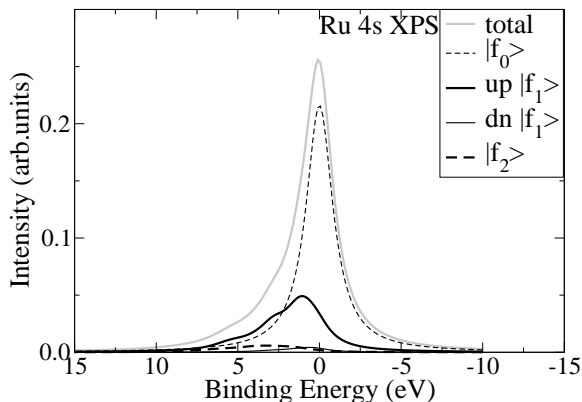

Figure 12: $4s$ XPS spectra in nonmagnetic ruthenium as a function of binding energy for the $4s$ down-spin core-hole.

IV. CONCLUDING REMARKS

We have developed an *ab initio* method to calculate the $3s$ and $4s$ core-level XPS spectra in ferromagnetic metals Ni, Co, and Fe, and in nonmagnetic metals Cu, V, and Ru. For the ferromagnetic metals, we have found that the spectral intensities are distributed in a wide range of binding energy with satellite or shoulder structures

for the up-spin channel, while the intensities are concentrated near the threshold with no satellite peak for the down-spin channel. The origin of such behavior has been explained in relation to the $3d$ band modified by the core-hole potential and the overlap integral between the final states and the ground state. Bound or quasi-bound states are formed by the core-hole potential, and the e-h excitations from such quasi-bound states to the unoccupied levels would usually give rise to satellite intensities. However, the presence of the quasi-bound state is not a sufficient condition to the presence of satellite; the d-band should be partially occupied in the ground state, and thereby the one-electron wave functions constituting the final states include the amplitudes of the unoccupied one-electron states in the ground state. If the d-band is fully occupied, the satellite intensity would not come out even in the presence of the bound state. Note that the satellite peak position has no direct relation to the $3s$ level exchange splitting; the LDA calculation gives such splittings as 0.7, 1.9, and 2.5 eV for Ni, Co, and Fe, respectively.

These results indicate that the presence of satellite is not directly related to the ferromagnetic ground state. We have clarified this point by calculating the spectra in nonmagnetic metals Cu, V, and Ru. For V and Ru, we have obtained shoulder structures in the XPS spectra, although the structure is rather small for Ru. The origin of these behaviors is the same as in the ferromagnetic metals. For Cu, only a symmetric peak is found with no structure, although the *localized* bound states are clearly formed below the bottom of the conduction band. This is because the $3d$ band is completely occupied in the ground state.

We have calculated the XPS spectra in Ni, Co, Fe, and Cu in good agreement with the experiment, while we could not find experimental XPS data for V and Ru. Acker et al. observed the satellite structures even in some Pauli paramagnetic Fe compounds,[8] The present results would provide an interpretation of their findings. Finally, as regards the L-edge spectra, experimental data for XPS spectra and the x-ray absorption spectra are accumulated, and *ab initio* approach has been tried.[26] The extension of the present method to the L-edge spectra is left in future study.

[1] P. W. Anderson, Phys. Rev. Lett. **18**, 1049 (1967).

[2] G. D. Mahan, Phys. Rev. **163**, 612 (1967).

[3] P. Noziéres and C. T. de Dominicis, Phys. Rev. **178**, 1097 (1969).

[4] S. Doniach and M. Sunjic, J. Phys. C **3**, 285 (1970).

[5] S. Hufner and G. W. Wetheim, Phys. Lett. **51A**, 301 (1975).

[6] L. A. Feldkamp and L. C. Davis, Phys. Rev. B **22**, 3644 (1980).

[7] C. S. Fadley and D. A. Shirley, Phys. Rev. A **2**, 1109 (1970).

[8] J. F. van Acker, Z. M. Stadnik, J. C. Fuggle, H. J. W. M. Hoekstra, K. H. J. Buschow, and G. Stroink, Phys. Rev. B **37**, 6827 (1988).

[9] F. U. Hillebrecht, R. Jungblut, and E. Kisker, Phys. Rev. Lett. **65**, 2450 (1990).

[10] D. G. Van Campen and L. E. Klebanoff, Phys. Rev. B **49**, 2040 (1994).

[11] Z. Xu, Y. Liu, and P. D. Johnson, Phys. Rev. B **51**, 7912 (1995).

[12] A. K. See and L. E. Klebanoff, Phys. Rev. B **51**, 7901 (1995).

[13] A. K. See and L. E. Klebanoff, Phys. Rev. B **51**, 11002 (1995).

[14] W. J. Lademan and L. E. Klebanoff, Phys. Rev. B **55**, 6766 (1997).

[15] I. N. Shabanova, N. V. Keller, V. A. Sosnov, and A. Z. Menshikov, J. Electron. Spectrosc. Relat. Phenom. **114-116**, 581 (2001).

[16] N. Kamakura, A. Kimura, T. Saitoh, O. Rader, K. S. An, and A. Kakizaki, Phys. Rev. B **73**, 094437 (2006).

[17] P. S. Bagus and J. V. Mallow, Chem. Phys. Lett. **228**, 695 (1994).

[18] S.-J. Oh, G.-H. Gweon, and J.-G. Park, Phys. Rev. Lett. **68**, 2850 (1992).

[19] M. Takahashi, J. Igarashi, and N. Hamada, Phys. Rev. B **78**, 155108 (2008).

[20] J. Friedel, Nuovo Cim. Suppl. **2**, 287 (1958).

[21] Y. Kakehashi, K. Becker, and P. Fulde, Phys. Rev. B **29**, 16 (1984).

[22] M. S. Hybertsen and S. G. Louie, Phys. Rev. B **34**, 5390 (1986).

[23] N. Hamada, M. Hwang, and A. J. Freeman, Phys. Rev. B **41**, 3620 (1990).

[24] A. Kotani and Y. Toyozawa, J. Phys. Soc. Jpn. **37**, 912 (1974).

[25] V. L. Morruzi, J. F. Janak, and A. R. Williams, *Calculated Electronic Properties of Metals* (Pergamon, New York, 1978).

[26] P. Kruger and C. R. Natoli, Phys. Rev. B **70**, 245120 (2004).